

# An Axial Output Relativistic Magnetron Fed by a Split Cathode and Magnetically Insulated by a Low-Power Solenoid

J. G. Leopold<sup>1</sup>, Member, IEEE, Ya. E. Krasik<sup>2</sup>, Fellow, IEEE, Y. Hadas,  
and E. Schamiloglu<sup>3</sup>, Fellow, IEEE

**Abstract**—One of the main difficulties in designing a relativistic magnetron producing high-power microwaves (HPMs) to be compact, is the power source required to feed the solenoid producing the axial magnetic field, which magnetically insulates the electron beam. This is because the diffusion of the magnetic field through the walls of the system is on the millisecond timescale. The latter requires high-power supplies and restricts the magnetron from operating repetitively. Using permanent magnets instead does not make the system sufficiently compact, because of the size and weight of the magnets and does not allow varying the magnetic field. We suggest a simple solution to this problem by cutting longitudinal slits through the entire magnetron anode system. With such slits, the magnetic field penetration is not restricted by the diffusion rate. Thus, one can apply a microsecond-timescale magnetic field produced by a solenoid powered by a considerably smaller power supply. We test this idea by using particle-in-cell (PIC) simulations of a magnetron for the axial output design suggested by Xu *et al.* (2018) fed by a split cathode (Leopold *et al.*, 2020). With a split cathode, the second major problem with relativistic magnetrons is alleviated—pulse shortening is avoided.

**Index Terms**—High-power microwave (HPM) generation, magnetrons.

## I. INTRODUCTION

RELATIVISTIC magnetrons have been of interest since the 1970s [1] as high-power microwave (HPM) sources and many ideas were realized to improve their efficiency [2]. These devices are the most promising HPM sources in terms of their microwave generation efficiency and compactness, but some problems need to be solved first. One of the problems

Manuscript received May 17, 2021; revised July 29, 2021; accepted August 15, 2021. Date of publication August 30, 2021; date of current version September 22, 2021. The work at the Technion was supported in part by the Office of Naval Research Global (ONRG) Grant No. N62909-21-1-2006 and in part by the Technion under grant 2029541. The work at the University of New Mexico was supported in part by the Air Force Office of Scientific Research (AFOSR) under Grant No. FA9550-19-1-0225 and in part by the Office of Naval Research (ONR) under Grant No. N00014-19-1-2155. The review of this article was arranged by Editor R. Letizia. (Corresponding author: J. G. Leopold.)

J. G. Leopold, Ya. E. Krasik, and Y. Hadas are with the Department of Physics, Technion–Israel Institute of Technology, Haifa 3200003, Israel (e-mail: leopoldjg@gmail.com).

E. Schamiloglu is with the Department of Electrical and Computer Engineering, The University of New Mexico, Albuquerque, NM 87131 USA (e-mail: eds@unm.edu).

Color versions of one or more figures in this article are available at <https://doi.org/10.1109/TED.2021.3105942>.

Digital Object Identifier 10.1109/TED.2021.3105942

that need solution is HPM pulse shortening caused by the explosively formed cathode plasma evolution [3], common to many HPM sources, and which was addressed by ideas such as the transparent cathode [4], the virtual cathode (VC) [5], and the VC with a magnetic mirror [6]. The transparent cathode used a solid cathode made up of a few conducting ribs, placed in front of each resonator, thus reducing the surface of the conductor involved in the explosive emission while increasing the coupling between the microwave field and the drifting electrons. The VC is based on the idea of the squeezed state of an electron beam [7], that is, the low-energy high-density electron charge trapped between two VCs. The disadvantage of producing a VC is that it requires increasing the radius of the tube containing the magnetron. A magnetic mirror is difficult to realize and requires an additional power supply to energize an additional mirror coil. Recently, a novel type of cathode, the split cathode was introduced and tested experimentally [8]. The split cathode consists of a cathode that is placed upstream and outside the magnetron and is connected by an axial rod to a reflector placed downstream from the magnetron. The annular electron beam emitted by the cathode emitter is trapped in the space between the cathode and the reflector and, at the same time, screens the rod from explosive plasma formation. The split cathode is a simple and practical way to realize a VC without the disadvantages mentioned regarding previous VC ideas. The operation of a split cathode as the electron source in a relativistic magnetron was recently experimentally confirmed and revealed that, indeed, using a split cathode mitigates pulse shortening [9].

The second problem needing solution is making the relativistic magnetron and its accompanying magnetic field-producing system compact. Diverting efficiently the microwaves produced in each radial magnetron resonator into the axial direction reduces the size of the magnetron. Such a scheme was realized successfully in a magnetron with diffraction output (MDO) with high efficiency [10]. Other axial output schemes are being pursued as well [11]. Nevertheless, the main obstacle making a relativistic magnetron system compact remains the size and weight of the uniform axial magnetic field producing system (0.2–0.5 T along a considerable length). This is typically produced by a pulsed solenoid forming a magnetic field on the millisecond timescale necessary for the magnetic field to diffuse through the conducting walls of the magnetron's anode. These long times require a high-power

supply and limit the repetition rate of magnetron operation. Modern permanent magnets can provide such fields, but the magnetron system is still too large and too heavy to be considered compact [12], [13]. Permanent magnets can also be incorporated into the magnetron vanes and the hollow cathode [14], but this compact arrangement is limited by the available magnetic field. Finally, permanent magnets do not allow for variability of the magnetic field amplitude.

In this article, we suggest a simple solution to considerably reduce the power required by the system supplying the insulating magnetic field.

## II. LOW-POWER SOLENOID SYSTEM

In this article, we propose to build the solenoid around a magnetron in which longitudinal slits have been cut through the entire radius of the entire magnetron anode structure. With slits, there is no restriction on the magnetic field's penetration rate, and a pulsed solenoid on the microsecond time scale can be used, which can be powered by a compact power supply. The magnetic field of a solenoid of length  $l$ , diameter  $D$ , and the total number of turns  $N$  is  $B = k\mu_0NI_{\max}/l$ , where  $k$  is the correction coefficient that accounts for the finite length of the solenoid [15], [16]. Here,  $I_{\max}$  is the maximal current amplitude for an almost periodic discharge circuit containing a storage capacitor of capacitance  $C$  and solenoid inductance  $L = \mu_0N^2\pi D^2/4l$ . Thus, for a capacitor charging voltage  $\varphi_{\text{ch}}$ , the magnetic field is  $B = 2k\varphi_{\text{ch}}(\mu_0C/\pi D^2l)^{1/2}$ . For instance, for  $\varphi_{\text{ch}} = 5$  kV for a capacitor  $C = 10$   $\mu\text{F}$  (storage energy of only 125 J), a 0.2-m-long, 0.12-m-diameter,  $k \approx 0.79$  solenoid will produce a magnetic field of 0.29 T. The inductance of a solenoid with 35 turns of 2 mm  $\times$  5 mm rectangular wires will be  $\sim 5.5$   $\mu\text{H}$ . Thus, the maximal current and the duration of the magnetic field will be  $\sim 6.7$  kA and  $\sim 23$   $\mu\text{s}$ , respectively. This type of solenoid is simple to manufacture and is expected to produce magnetic fields in the range of 0.2–1 T. The pulsed power supply of such a solenoid can be made compact and lightweight. Note that one can cover the surface of the slits with thin conducting material. Indeed, assuming a conducting material of  $\sim 5$  times smaller thickness than the skin depth  $\delta = (\rho T/\pi)^{1/2}$ , where  $\rho$  is the resistivity of the material and  $T$  is the period of the magnetic field, the latter will penetrate almost without decay. For the example considered above and copper, the thickness of the foil should be not more than 90  $\mu\text{m}$ .

This idea is trivial and will be tested experimentally with a magnetron in the near future. To keep the symmetry of the magnetron, more than one longitudinal slit is needed, which means that the magnetron anode has to be put together from separate unconnected parts. Since the magnetron anode becomes an open system, to fulfill vacuum requirements, it can be placed inside a dielectric or ceramic tube around which the solenoid windings are placed, while the magnetron with longitudinal slits is held inside it. These technical problems can be solved in practice.

Assuming that the available axial magnetic field supplied by the low-power solenoid system remains the same as with high power, we test, using particle-in-cell (PIC) simulations, the effect of such longitudinal slits on the operation of a magnetron.

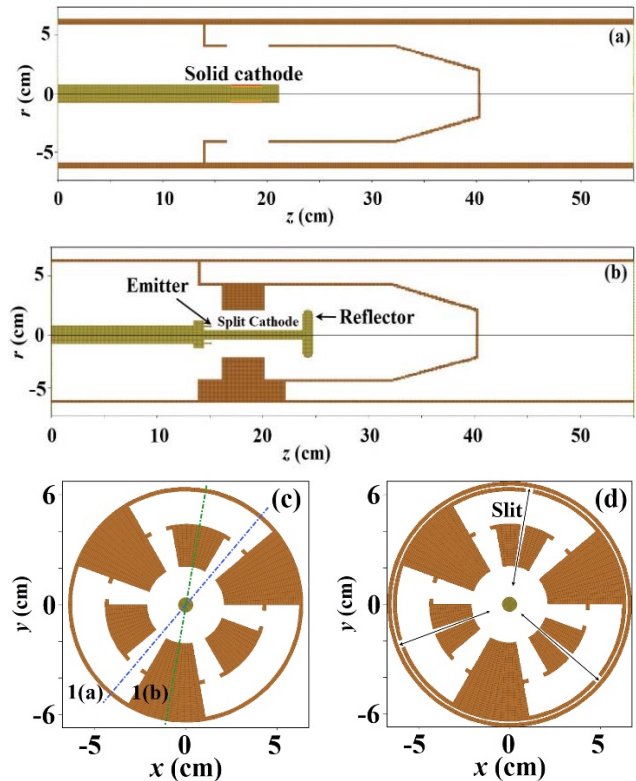


Fig. 1. (a) Cross section of a magnetron fed by a solid cathode in the plane showing two opposite resonators and axial output channels [see line designated by 1(a) in frame (c)]. (b) Cross section across two opposite vanes [see line designated by 1(b) in frame (c)] with a split cathode replacing the solid cathode. (c) Transverse cross section of the magnetron at its axial center, showing the sectorial separators. (d) Same as (c) but with three longitudinal slits.

## III. PIC SIMULATIONS

We use the MAGIC [16] PIC code to simulate a six-vane magnetron with an all cavity axial output design suggested in [11]. The difference in this design compared to other axial output designs is that the downstream flowing axial current, if it exists, does not appear in the space where microwaves are routed. We test the performance of a split cathode [8] in such a design. Finally, we add longitudinal slits to test their effect on the operation of this magnetron. The axial output magnetron is a compact system by design. The split cathode solves the problem of pulse shortening [9] and mitigates axial leakage current, while the incorporation of slits allows the use of a lightweight solenoid and power supply, increasing the overall efficiency of the system.

We present simulation results for an axial output 40-mm-long (21-mm/42-mm inner/outer anode radii) A6 magnetron for the three configurations shown in Fig. 1. The magnetron design includes a cylindrical tube followed by a closed conical section surrounding the magnetron and separating it from the electromagnetic radiation region [see Fig. 1(a) and (b)]. Three vanes are continued radially into the space outside this tube and reach the outer radius of the system, which makes them, together with the outer tube, to act like straps [see Fig. 1(c)]. The space outside the magnetron, which we call a radiator, becomes divided into three sectors. The axial length and azimuthal angle of these sectorial dividers are parameters,

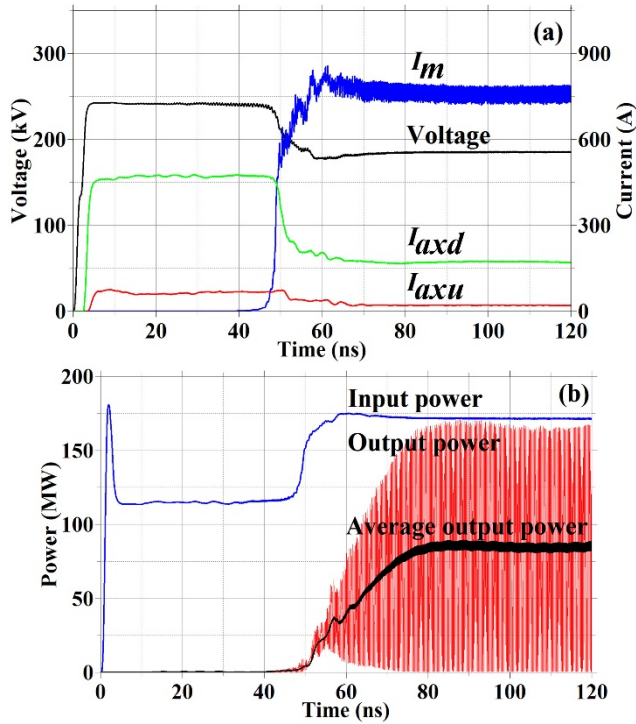


Fig. 2. PIC simulation results for a magnetron fed by a solid cathode [see Fig. 1(a)]. Time dependence of (a) voltage at the upstream open boundary, the axial current flowing in the upstream ( $I_{axu}$ ) and downstream ( $I_{axd}$ ) directions, and the magnetron current ( $I_m$ ). (b) Input power, the output power, and the average output power.

which need optimization [11], which we have not performed for this article.

In Fig. 1(a), the electron source is a solid cathode, while, in Fig. 1(b), it is a split cathode consisting of a cathode holding an annular emitter, a reflector, and a connecting nonemitting rod. In Fig. 1(d), three  $4^\circ$  angular slits are cut radially at the center angle of three vanes. The slits cut the entire magnetron anode and the inner tube of the radiator (but not the cover of the conical section). We cut three slits (although one would be sufficient for magnetic field penetration), so as not to introduce an asymmetry in the magnetron structure. For all cases studied, we fix the axial uniform magnetic field at 0.25 T. The outer tube of the system is now open, and here, we assume that a conducting closed tube exists at a 1-mm distance [see Fig. 1(d)]. In practice, one can enclose the vacuum tube with a ceramic or dielectric insulator and wind the solenoid around its surface, and one can also cover the slits with a thin conducting foil.

For all cases, on the upstream open boundary, we apply a voltage of 300 kV rising in 1 ns, which changes through the simulation time reflecting the impedance change of the system. For a solid cathode [see Fig. 1(a)], we assume that the central cylinder emits electrons by space-charge-limited emission along 30 mm at the center of the magnetron anode. In Fig. 2, we present the PIC simulation results for this solid cathode.

As the voltage increases, emission starts, and axial currents develop in both directions. The electrons approach the anode during  $\sim 50$  ns and the magnetron current reaches  $\sim 760$  A at

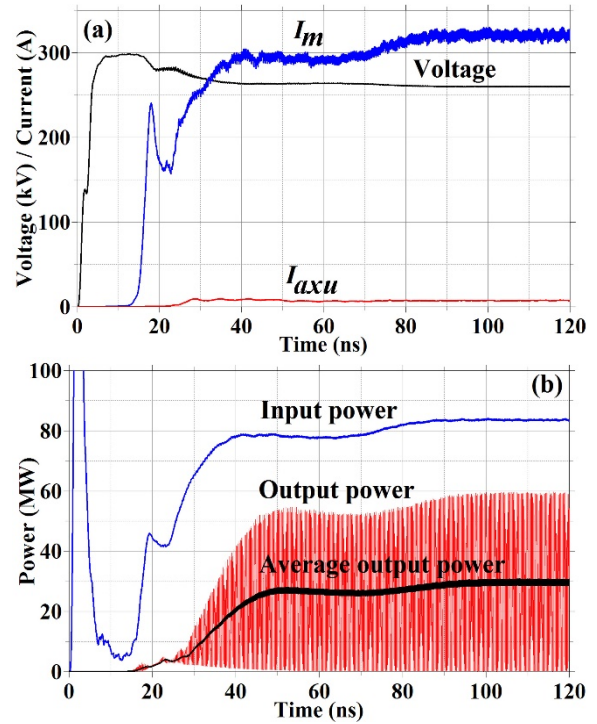


Fig. 3. (a) and (b) are the same as Fig. 2(a) and (b), respectively, except that the results are for a split cathode fed magnetron [see Fig. 1(b)].

$\sim 65$  ns [see Fig. 2(a)]. This affects the impedance of the system so that the voltage and both axial currents decrease [17]. For the parameters used, the input power of this system stabilizes at  $\sim 172$  MW and the average power at  $\sim 86$  MW with an average efficiency of  $\sim 50\%$  [see Fig. 2(b)].

Our purpose at this point is not to maximize the output power and efficiency but to test the split cathode and the effect of the magnetic field penetrating slits. In Fig. 3, simulation results for the operation of the same magnetron with a split cathode [see Fig. 1(b)] are presented. For this configuration, the steady-state voltage ( $\sim 260$  kV) is higher than that obtained for the solid cathode case [ $\sim 186$  kV in Fig. 3(a)]. This is because the total current (the sum of the magnetron current and the axial currents) is smaller (the magnetron current reaches  $\sim 320$  A compared to  $\sim 760$  A for the solid cathode case). This is not surprising because the emitted current of the annular cathode is limited by its relatively small area compared to the large area solid cathode. It is possible to increase the current by replacing the reflector with a second cathode. This will not add plasma to the magnetron interaction region, but it can increase the current by at most a factor of 2. In addition, one could increase the input voltage to the limit that not too much current flows axially. The downstream axial current is negligible and is not shown in Fig. 3(a), and the axial upstream current escaping above the cathode is small. The different impedance of this configuration dictates that the input power  $\sim 83$  MW [see Fig. 3(b)] is about half of that obtained for the solid cathode case [see Fig. 2(b)], and the average efficiency is  $\sim 36\%$ . This value is smaller than that for the solid cathode case.

In Fig. 4, we present simulation results for the axial output magnetron fed by a split cathode and with three longitudinal slits cut in its anode parts [see Fig. 1(d)]. When we compare

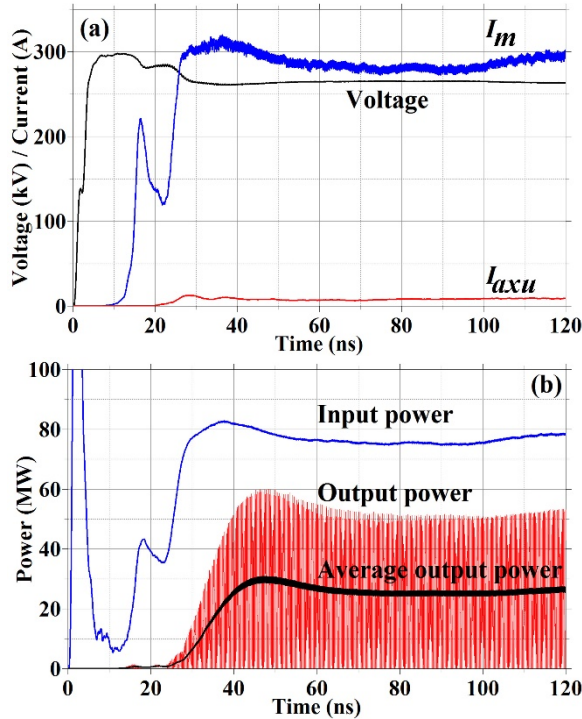


Fig. 4. (a) and (b) are the same as Fig. 2(a) and (b), respectively, except that the results are for a split cathode fed magnetron [see Fig. 1(d)].

Fig. 4(a) with Fig. 3(a), we see that the long-time voltage is slightly higher and the magnetron current is lower. The upstream axial currents are small in both cases, and the downstream axial currents (overflow above the reflector) are negligible. In Fig. 4(b), the input power, the output power, and its average are all slightly lower than in Fig. 3(b). We also measure the power lost in the space between the magnetron's outer tube (with open slits) and the tube enclosing the system [see Fig. 1(d)], which is, on average,  $\sim 2$  MW. Nevertheless, at  $\sim 120$  ns, the input power reaches  $\sim 78$  MW, and the average output power reaches  $\sim 27$  MW, which gives  $\sim 35\%$  efficiency, almost the same as the efficiency in the absence of slits. We should point out that, when the slits are placed along the center of one of the magnetron resonators, introducing an asymmetry into the structure, the magnetron stops radiating microwaves as one should expect.

The simulations show that all three magnetron configurations operate in the  $\pi$ -mode (see Fig. 5).

In Fig. 5(a)–(c), contours of the azimuthal and, in Fig. 5(d)–(f), the radial components of the electric field are drawn at  $\sim 120$  ns. Fig. 5(a) and (d) are for the solid cathode fed magnetron, Fig. 5(b) and (e) for a split cathode, and Fig. 5(c) and (f) for a split cathode and longitudinal slits. Both  $E_\theta$  and  $E_r$  are much stronger when a solid cathode is used, which is the result of the higher input power compared to when a split cathode is used (by almost a factor of 2). Very little difference is seen when longitudinal slits are added [compare Fig. 5(b) to Fig. 5(c) and Fig. 5(e) to Fig. 5(f)]. In Fig. 6,  $E_\theta$  and  $E_r$  are depicted along radial lines at the center of each of three nonadjacent magnetron cavities (where the fields are negative; see Fig. 5) at the axial center of the magnetron for the split cathode fed magnetrons when no

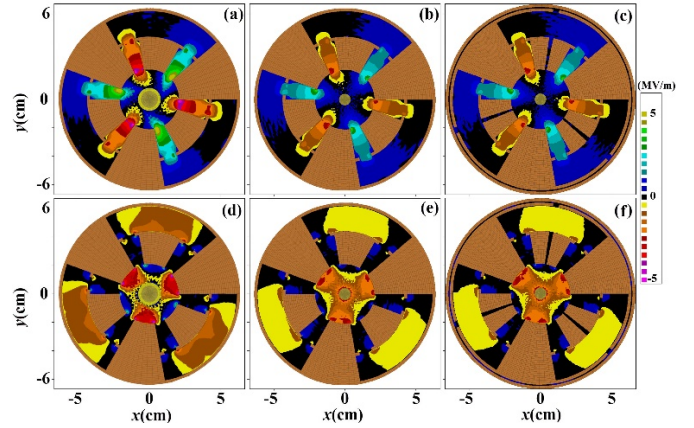


Fig. 5. Contours of  $E_\theta$  [(a)–(c)] and  $E_r$  [(e)–(f)] in the  $[x, y]$  plane at the longitudinal ( $z$ ) center of the magnetron at  $\sim 120$  ns for the solid cathode [(a) and (d)], the split cathode [(b) and (e)], and the split cathode and longitudinal anode slits [(c) and (f)].

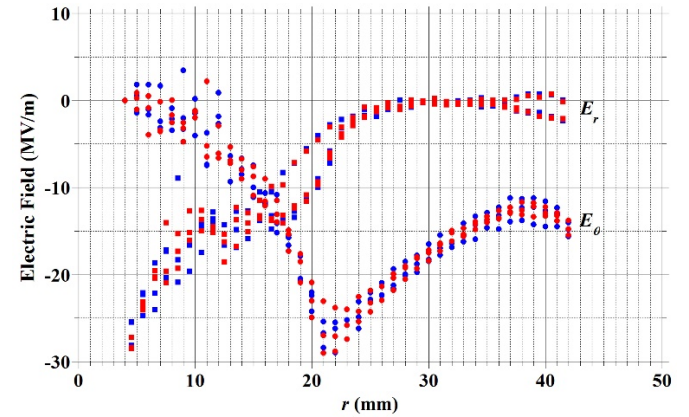


Fig. 6. Electric field components  $E_\theta$  (full circles) and  $E_r$  (full squares) along radial lines from the axis to the magnetron's anode outer radius (42 mm) lying at the cavity's central angle at  $\sim 120$  ns. For the SpltC case, results are colored blue, whereas, for the SpltC-ASlts case, red. Note that the rod radius is 4 mm and the magnetron anode's inner radius is 21 mm.

longitudinal slits are cut (SpltC) compared to the case with such slits (SpltC-ASlts). The results are spread, but they lie on a band, which is the result of the finite mesh.

There is no distinguishable difference between the two cases considered, which indicates that the power exchange between the electrons and the microwaves is not affected by the introduction of slits.

In Fig. 7, contours of the electron density are drawn for the three compared cases at  $\sim 120$  ns. Fig. 7(a)–(c) corresponds to Fig. 5(a)–(c), respectively.

There is no significant effect when the magnetron fed by a split cathode is with longitudinal slits. Note that, for the solid cathode case, the spokes are different and perhaps more distinct. The screening of the rod by the electron cloud in Fig. 7(b) and (c) is evident.

We have conducted an eigenmode analysis of the three magnetrons systems. The analysis is performed by the MAGIC PIC code in a closed system (no open boundaries) for all three configurations ascertained to have the same volume. In the frequency range of 1.5–3.0 GHz, the same  $\pi$ -mode is obtained with the same frequency (2.23 GHz) and no other modes

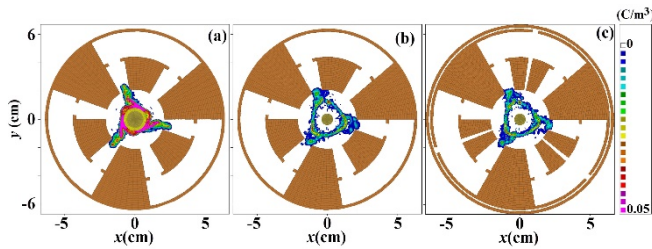


Fig. 7. Contours of electron densities at  $\sim 120$  ns for (a) solid cathode, (b) split cathode fed magnetrons, and (c) when for the latter, longitudinal slits are cut.

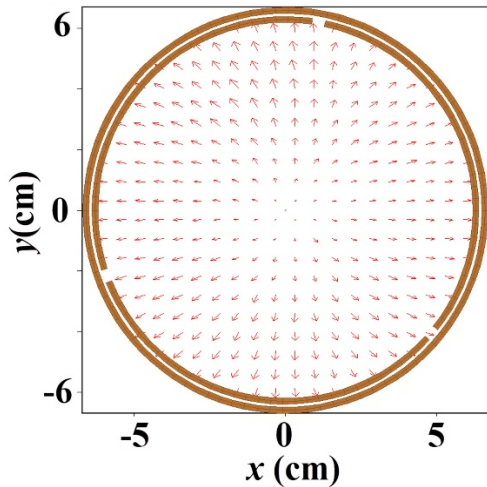


Fig. 8. Vector plot showing the distribution of the orientation and relative amplitude of the electric field at  $\sim 120$  ns in the plane of the downstream output boundary of the magnetron system cut with longitudinal anode slits and fed by a split cathode.

for all three cases. For the  $\pi$ -mode of the simulated systems in Fig. 5, the frequencies for all three cases were also the same, 1.925 GHz. These results are an additional indication that the introduction of the slits does not introduce disruptions.

The axial output design converts the microwaves produced in the magnetron into a  $TM_{01}$  mode at the downstream open boundary. This is seen in Fig. 8 that depicts a vector plot showing the orientation and relative amplitude of the electric fields in this plane for the magnetron system with longitudinal slits and fed by a split cathode. For the other two cases, the corresponding vector plots are very similar to the distribution seen in Fig. 8.  $E_\theta$  in Fig. 5 and  $E_r$  in Fig. 8 oscillate with a frequency of  $\sim 1.925$  GHz for all three configurations.

#### IV. SUMMARY

We have demonstrated using PIC simulations that a split cathode, which solves the problem of pulse shortening, can also replace a solid cathode in an axial output magnetron. Adding longitudinal slits to allow more rapid magnetic field penetration affects the electronic efficiency of the magnetron very little. With a split cathode, to obtain an absolute output power comparable to that obtained with the corresponding solid cathode, one needs to increase the input power by a factor of  $\sim 2$ , which can be achieved either by a voltage increase or adding a second cathode replacing the reflector. We demonstrate that the introduction of slits for magnetic field

penetration does not affect the operation of an axial output magnetron, which, in turn, allows for considerable reduction of the system size and weight, and a concomitant increase in system efficiency. The electromagnetic perturbation of the slits can be completely eliminated by covering their openings using thin copper foils without affecting the magnetic field's diffusion rate.

#### ACKNOWLEDGMENT

The authors would like to thank Dr. Y. Bliokh for fruitful discussions clarifying some of the physical ideas of this article.

#### REFERENCES

- [1] G. Bekefi and T. J. Orzechowski, "Giant microwave bursts emitted from a field-emission, relativistic-electron-beam magnetron," *Phys. Rev. Lett.*, vol. 37, no. 6, pp. 82–379, Aug. 1976, doi: [10.1103/PhysRevLett.37.379](https://doi.org/10.1103/PhysRevLett.37.379).
- [2] D. Andreev, A. Kuskov, and E. Schamiloglu, "Review of the relativistic magnetron," *Matter Radiat. Extremes*, vol. 44, Apr. 2019, Art. no. 067201, doi: [10.1063/1.5100028](https://doi.org/10.1063/1.5100028).
- [3] J. Benford and G. Benford, "Survey of pulse shortening in high-power microwave sources," *IEEE Trans. Plasma Sci.*, vol. 25, no. 2, pp. 311–317, Apr. 1997, doi: [10.1109/27.602505](https://doi.org/10.1109/27.602505).
- [4] M. Fuks and E. Schamiloglu, "Rapid start of oscillations in a magnetron with a 'transparent' cathode," *Phys. Rev. Lett.*, vol. 95, no. 20, Nov. 2005, Art. no. 205101, doi: [10.1103/PhysRevLett.95.205101](https://doi.org/10.1103/PhysRevLett.95.205101).
- [5] M. I. Fuks, S. Prasad, and E. Schamiloglu, "Efficient magnetron with a virtual cathode," *IEEE Trans. Plasma Sci.*, vol. 44, no. 8, pp. 1298–1302, Aug. 2016, doi: [10.1109/TPS.2016.2525921](https://doi.org/10.1109/TPS.2016.2525921).
- [6] M. I. Fuks and E. Schamiloglu, "Application of a magnetic mirror to increase total efficiency in relativistic magnetrons," *Phys. Rev. Lett.*, vol. 122, no. 22, Jun. 2019, Art. no. 224801, doi: [10.1103/PhysRevLett.122.224801](https://doi.org/10.1103/PhysRevLett.122.224801).
- [7] A. M. Ignatov and V. P. Tarakanov, "Squeezed state of high-current electron beam," *Phys. Plasmas*, vol. 1, pp. 741–744, Mar. 1994, doi: [10.1063/1.870819](https://doi.org/10.1063/1.870819).
- [8] J. G. Leopold, Ya. E. Krasik, Y. P. Bliokh, and E. Schamiloglu, "Producing a magnetized low energy, high electron charge density state using a split cathode," *Phys. Plasmas*, vol. 27, 2020, Art. no. 103102, doi: [10.1063/5.0022115](https://doi.org/10.1063/5.0022115).
- [9] J. G. Leopold *et al.*, "Experimental and numerical study of a split cathode fed relativistic magnetron," *J. Appl. Phys.*, vol. 130, no. 3, Jul. 2021, Art. no. 034501, doi: [10.1063/5.0055118](https://doi.org/10.1063/5.0055118).
- [10] C. Leach, S. Prasad, M. I. Fuks, C. J. Buchenauer, J. McConaha, and E. Schamiloglu, "Experimental demonstration of a high-efficiency relativistic magnetron with diffraction output with spherical cathode end-caps," *IEEE Trans. Plasma Sci.*, vol. 45, no. 2, pp. 282–288, Feb. 2017, doi: [10.1109/TPS.2016.2644625](https://doi.org/10.1109/TPS.2016.2644625).
- [11] S. Xu, L. Lei, F. Qin, and D. Wang, "Compact, high power and high efficiency relativistic magnetron with L-band all cavity axial extraction," *Phys. Plasmas*, vol. 25, 2018, Art. no. 083301, doi: [10.1063/1.5041860](https://doi.org/10.1063/1.5041860).
- [12] W. Li, J. Zhang, Z.-Q. Li, and J.-H. Yang, "A portable high power microwave source with permanent magnets," *Phys. Plasmas*, vol. 23, May 2016, Art. no. 063109, doi: [10.1063/1.4953602](https://doi.org/10.1063/1.4953602).
- [13] A. J. Sandoval. *An Experimental Verification of A6 Magnetron With Permanent Magnet*. M.S. thesis, Electrical and Computer Engineering Dept. University of New Mexico. Albuquerque, NM. Apr. 2018. [Online]. Available: [https://digitalrepository.unm.edu/ece\\_etds/400/](https://digitalrepository.unm.edu/ece_etds/400/)
- [14] Ya. E. Krasik, J. G. Leopold, and U. Dai, "A relativistic magnetron operated with permanent magnets," *IEEE Trans. Plasma Sci.*, vol. 47, no. 8, pp. 3997–4005, Aug. 2019, doi: [10.1109/TPS.2019.2926535](https://doi.org/10.1109/TPS.2019.2926535).
- [15] M. W. Kennedy, S. Aktar, J. A. Bakken, and R. E. Aune, "Empirical verification of a short-coil correction factor," *IEEE Trans. Ind. Electr.*, vol. 61, no. 5, pp. 2573–2583, May 2014, doi: [10.1109/TIE.2013.2281168](https://doi.org/10.1109/TIE.2013.2281168).
- [16] B. Goplen, L. Ludeking, D. Smith, and G. Warren, "User-configurable MAGIC for electromagnetic PIC calculations," *Comput. Phys. Commun.*, vol. 87, nos. 1–2, pp. 54–86, May 1995, doi: [10.1016/0010-4655\(95\)00010-D](https://doi.org/10.1016/0010-4655(95)00010-D).
- [17] J. G. Leopold, A. S. Shlapakovski, A. Sayapin, and Ya. E. Krasik, "Revisiting power flow and pulse shortening in a relativistic magnetron," *IEEE Trans. Plasma Sci.*, vol. 43, no. 9, pp. 3168–3175, Sep. 2015, doi: [10.1109/TPS.2015.2463717](https://doi.org/10.1109/TPS.2015.2463717).